BODIPY-based ratiometric fluorescent probes for the sensitive and selective sensing of cyanide ions

5 AUTHORS, INCLUDING:

Jingtuo Zhang

Michigan Technological University

15 PUBLICATIONS   **232** CITATIONS

BODIPY-based ratiometric fluorescent probes for the sensitive and selective sensing of cyanide ions†
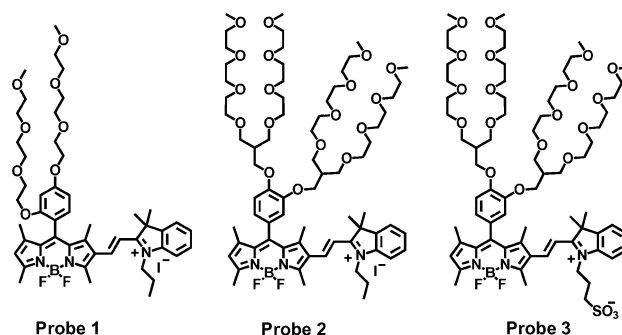
Jingtuo Zhang,[a] Shilei Zhu,[a] Loredana Valenzano,[a] Fen-Tair Luo[b] and Haiying Liu*[a]

Three BODIPY-based ratiometric fluorescent probes (1, 2 and 3), with two being highly soluble in aqueous solution, were prepared by the condensation of 2-formyl-BODIPY dyes with 2,3,3-trimethyl-1-propyl-3*H*-indolium iodide and 2,3,3-trimethyl-1-(3-sulfonatepropyl)-3*H*-indolium for the selective and sensitive ratiometric fluorescent responses to cyanide ions.

Cyanide is a well-known highly toxic substance and is very harmful to the human health.[1] A small amount of cyanide can result in extremely lethal poisoning, which is caused by the inhibition of cellular respiration in living creatures *via* its binding to a heme unit in the active site of cytochrome c when it is absorbed through the gastrointestinal track, skin or lungs.[2,3] As a result, any accidental release of cyanide salts from industries involved in gold mining, electroplating, metallurgy and the synthesis of nylon and other synthetic fibers and resins can cause serious environmental disasters,[4] especially under potential terrorist threats. Therefore, it is highly desirable to develop sensitive, selective and quick detection methods for toxic cyanide anions. Fluorescent probes have shown many promising advantages, including high sensitivity, low cost, fast responses and easy operation, for potential *in vitro* assay and *in vivo* imaging applications among the different chemical sensing approaches for cyanide ions.[5,6] These fluorescent probes are mainly based on the benzil rearrangement reaction,[5] nucleophilic addition,[7,8] hydrogen-bonding interactions,[9,10] cyanide complexation/addition,[11] and coordination of copper ions with cyanide[12,13] for sensing applications. However, most of these organic dyes are not soluble in aqueous solution, and there is still a need to address some limitations concerning the sensitivity, selectivity, longer wavelength emissions, and compatibility within an aqueous environment.

In this communication, we chose BODIPY dyes as the fluorescent transducers to develop three ratiometric fluorescent

probes (**1–3**) (Scheme 1) for the highly sensitive and selective sensing of cyanide ions, because the BODIPY dyes possess many advantages, such as high quantum yields and large extinction coefficients and easy tuning for longer wavelength emissions.[14–17] Fluorescent probe **1** was used to systematically study its response mechanism to cyanide ions by using ^{1}H NMR, mass spectrometry, absorption and fluorescence spectrometry, because of its structural simplicity with tri(ethylene glycol)methyl ether residues at the *meso*-position of BODIPY dye. For practical applications, the highly water-soluble fluorescent probe **3** was prepared to sensitively detect cyanide ions by introducing branched oligo(ethylene glycol)methyl ether residues and propanesulfonate to the BODIPY dye. Fluorescent probe **2** was used as a control to demonstrate the importance of the propanesulfonate residue in probe **3**. The propanesulfonate residue enhances the water solubility of the reaction product of the fluorescent probe with cyanide ions in order to achieve the sensitive detection of cyanide ions without any precipitation of probe **3**. The fluorescent probes show fast ratiometric fluorescent responses to cyanide ions with a dramatic fluorescence color change from red to green accompanying a significant increase in fluorescent intensity. This response results from the addition reaction of the cyanide ions with the iminium ions of the probe, which disrupts the π-conjugation between the BODIPY core and indole moiety, leading to significant dual color and fluorescence changes (Scheme 2).

[a]Department of Chemistry, Michigan Technological University, 1400 Townsend Drive, Houghton, MI, 49931, USA. E-mail: hyliu@mtu.edu; Fax: +1 9064872061; Tel: +1 9064873451

[b]Institute of Chemistry, Academia Sinica, Taipei, Taiwan, 11529, Republic of China

† Electronic Supplementary Information (ESI) available: synthesis, characterization and optical properties of the BODIPY dyes. See DOI: 10.1039/c2ra22205a
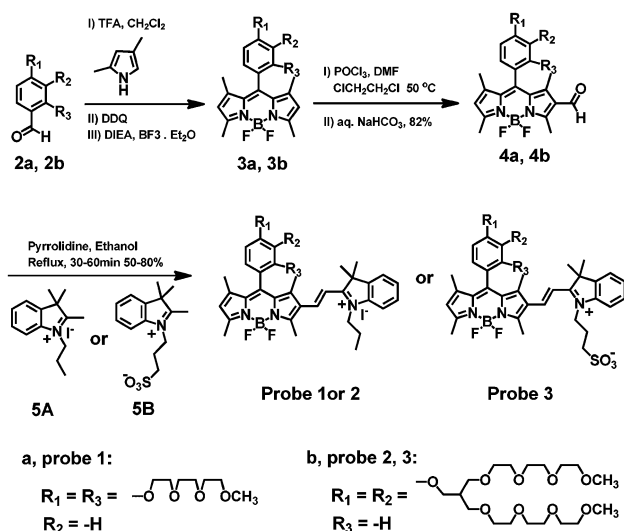
Scheme 1 BODIPY-based fluorescent probes for the detection of cyanide ions.
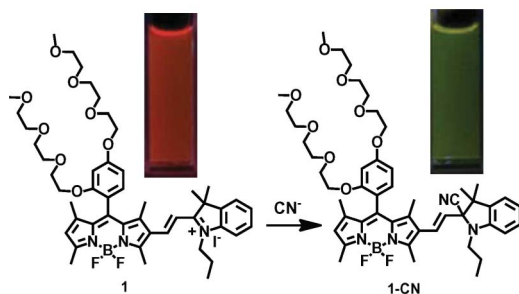
Scheme 2 Ratiometric fluorescent response of probe **1** to cyanide ions, with a dramatic fluorescence color change from red to green.

The strategy to prepare the fluorescent probes is outlined in Scheme 3. Use of an *ortho*-substituent group of tri(ethylene glycol)methyl ether on the *meso*-phenyl ring of BODIPY dye was used to increase the fluorescence quantum yield and hydrophilic property of the BODIPY dye.[18] BODIPY dyes (**3a**, **3b**) were prepared *via* the condensation of the benzaldehyde derivatives (**2a**, **2b**) with 2,4-dimethylpyrrole according to the reported procedure.[18–20] The 2-formyl-BODIPY dyes (**4a**, **4b**) were prepared by the Vilsmeier–Haack reaction of BODIPY dyes **3a** and **3b**, respectively.[19] Fluorescent probes **1**–**3** were readily prepared by the condensation reactions of the 2-formyl-BODIPY dyes (**4a**, **4b**) with 2,3,3-trimethyl-1-propyl-3*H*-indolium iodide (**5A**) or 2,3,3-trimethyl-1-(3-sulfonatepropyl)-3*H*-indolium (**5B**) in ethanol solution under reflux conditions (Scheme 3). All compounds have been characterized by ^{1}H NMR, ^{13}C NMR, and high-resolution mass spectroscopy (see the ESI†).

BODIPY dye **3a** shows absorption and emission peaks at 504 nm and 513 nm, respectively, and possesses a high fluorescence quantum yield of 92% in methylene chloride solution. 2-Formyl-BODIPY dye **4a** displays a lower fluorescence quantum yield and shows a slight blue shift (by 9 nm) in absorption compared to

BODIPY dye **3a** (see Fig. S21 in the ESI†). Fluorescent probe **1** exhibits two emission peaks at 515 nm and 605 nm (see Fig. S22 in the ESI†). The emission peak at 515 nm likely arises from the steric hindrance between the methyl groups of the BODIPY core at the 1,3-positions and the vinylic protons, which makes BODIPY core and indole moiety slightly nonplanar. This steric hindrance is further confirmed by the broad absorption peak of the probe (see Fig. S22 in the ESI†). Fluorescent probes **2** and **3** display similar optical properties in Tris buffer (10 mM, pH 9.3) as fluorescent probe **1** (see Table S2 in the ESI†).

We studied the concentration-dependent changes of the fluorescence and absorption spectra of probe **1** in the absence and presence of different equivalents of cyanide ions (Fig. 1 and 3). Addition of sodium cyanide results in the appearance of a new peak at 555 nm, and a drastic decrease in the peak at 605 nm. The new peak increases considerably with the gradual addition of cyanide ions, and a well-defined isoemissive point shows up at 598 nm (Fig. 1). 4.5 equivalents of cyanide ions is sufficient to make the reaction complete, showing that the probe is highly reactive towards cyanide ions. There is an up to 17-fold increase in the fluorescence ratio (I_{555}/I_{605}) in the presence of 4.5 equivalents of cyanide ions (Fig. 1). The detection limit ($S/N = 3$) was calculated to be 0.5 μM with a linear ratio response (I_{555}/I_{605}) of the fluorescence intensity at 555 nm and 605 nm to cyanide concentration ranging from 5.0 μM to 50.0 μM (Fig. 1, inset). Nucleophilic addition of the cyanide anion to the iminium ion causes the indole conjugation to the BODIPY core in probe **1** to break, resulting in significant dual color and fluorescence changes. Fluorescent probe **3** shows a highly sensitive response to cyanide ions with lower detection limit of 0.1 μM, significant decrease of emission peak at 600 nm, and appearance of a new emission peak at 550 nm in 10 mM Tris buffer (pH 9.3) (please see Fig. S34 in ESI†). A very good linear ratio response (I_{550}/I_{600}) of the fluorescence intensity at 550 nm and 600 nm to cyanide concentration was observed ranging from 0.5 μM to 50.0 μM in 10 mM Tris buffer (pH 9.3) (Fig. 2), which indicates that probe **3** has a potential useful application in the quantitative

Scheme 3 Synthetic route to BODIPY-based fluorescent probes **1**–**3**.
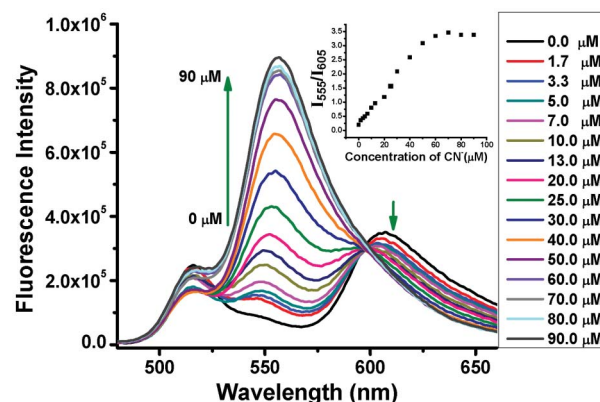

Fig. 1 Fluorescence spectra of fluorescent probe **1** (20 μM) in the absence and presence of different amounts of cyanide ions in a mixed solution of CH_3CN and Tris buffer (10 mM, pH = 9.3) (9 : 1, v/v). Inset: plot of the fluorescent intensity ratio change at 555 nm and 605 nm (I_{555}/I_{605}) of the fluorescent probe **1** upon titration of cyanide ions.
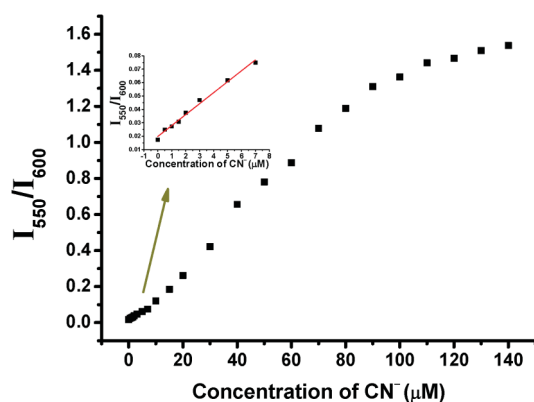
Fig. 2 Fluorescent intensity ratio changes at 550 nm and 600 nm (I_{550}/I_{600}) of the fluorescent probe **3** (20 µM) upon titration of cyanide ions in Tris buffer (10 mM, pH 9.3) solution.

detection of cyanide ions in aqueous solution. Addition of cyanide ions to probe **2** in Tris buffer (pH 9.3) resulted in similar fluorescence ratio responses to cyanide with poor linearity of the fluorescence ratio to cyanide concentration as the precipitation of the reaction product was observed due to the lack of charge repulsion of the neutral reaction product. These results indicate that the propanesulfonate residue in probe **3** plays a very important role in enhancing the water solubility of the reaction product of the fluorescent probe with cyanide ions, and prevents the dye from aggregating *via* charge repulsion between the propansulfonate groups for sensitive detection of cyanide ions.

Fig. 3 shows the absorption spectral changes of fluorescent probe **1** upon addition of cyanide ions in a mixed solution of CH_3CN–Tris buffer (10 mM pH = 9.3, 9 : 1, v/v). The gradual addition of cyanide ions to probe **1** also causes the emergence of a new absorption band at 521 nm, and significantly decreases the absorption band at 564 nm, which completely disappears with the
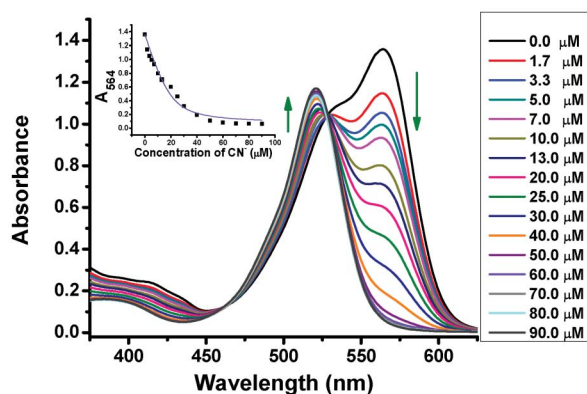

Fig. 3 Absorption spectra of probe **1** (20 µM) in the absence and presence of different amounts of cyanide ions in a mixed solution of CH_3CN–Tris buffer (10 mM pH = 9.3, 9 : 1, v/v). Inset: plot of absorbance change (A_{564}) of probe **1** upon addition of cyanide ions, where the line is the non-linear fitting curve obtained assuming a 1 : 1 reaction of the probe **1** with cyanide ions.

addition of 4.5 equivalents of cyanide ions (Fig. 3). A clean isosbestic point at 528 nm showed an interconversion into single distinct chemical species during the titration. This 1 : 1 stoichiometry was further confirmed by a good non-linear fitting of the titration data at 564 nm by assuming a 1 : 1 association between probe **1** and cyanide (Fig. 3 inset). The apparent association constant was determined to be 3.3×10^5 M^{-1} (see the ESI†). Probes **2** and **3** display similar absorption responses to cyanide ions in 10 mM Tris buffer (pH 9.3) (Fig. S29 and S35 in ESI†).

In order to shed light on the interesting absorption and emission features of fluorescent probe **1** and the reaction product **1**-CN, we investigated their structures by using density functional theory (DFT) and time-dependent DFT (TD-DFT) computational approaches (see ESI†) with the Gaussian 09 program.[21] Fig. 4 shows the optimized geometries for both structures. In probe **1**, the expected steric hindrance is confirmed and it translates to a slightly non-planar conformation of the structure (Fig. 4). The DFT and TD-DFT optimized structures of probe **1** and the reaction production **1**-CN show that probe **1** possesses a conjugated sp^2 hybridized carbon bond between the BODIPY core and indole group, while a sp^3 hybridized carbon in the reaction product **1**-CN is perpendicular to the BODIPY core (Fig. 4). A significant structure difference between probe **1** and the reaction product **1**-CN results in considerable difference in their π-conjugations. As a result, the electron densities of the LUMO of **1**-CN are only located on the BODIPY core, while those of probe **1** are spread over the BODIPY core through the indole moiety. The fluorescence enhancement of the reaction product **1**-CN arises from the prevention of internal charge transfer (ICT) between the BODIPY core and the indole moiety because of the conjugation disruption between the BODIPY core and indole group *via* the sp^3 hybridized carbon. A detailed understanding regarding the absorption and emission blue shift upon the formation of **1**-CN can be obtained *via* TD-DFT calculations as well. The lowest singlet electronic transitions of both probe **1** and reaction product **1**-CN are mainly contributed by the HOMO–LUMO transitions (see the ESI†). The calculated energy gap of probe **1** is 2.25 eV (551 nm) whereas the gap of **1**-CN is 2.45 eV (505 nm). This energy gap difference gives a 44 nm blue-shift in the absorption bands, which is in excellent agreement with the experimental data (43 nm).
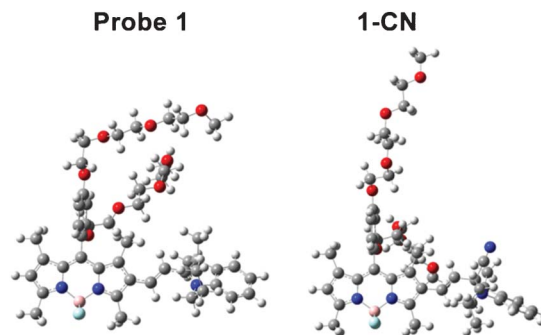

Fig. 4 Optimized structures of probe **1** and reaction product **1**-CN as obtained from TD-DFT calculations.
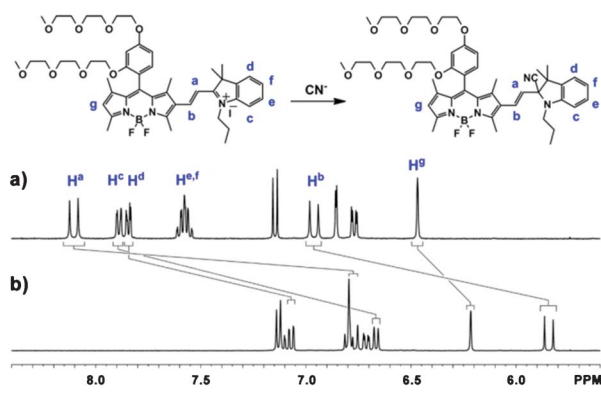
Fig. 5 ^{1}H NMR spectra of probe **1** (10 mM) in the absence (a) and presence (b) of cyanide ions (one equivalent) in DMSO-d_6 solution at room temperature.

We used ^{1}H NMR and mass spectroscopy to investigate the potential interaction mechanism of probe **1** with cyanide ions. A FAB-MS spectrometric analysis of the fluorescent probe treated with CN$^-$ in aqueous solution showed signals assignable to the formation of the **1**-CN adduct (m/z, 886.49). We also studied and compared the ^{1}H NMR spectra of fluorescent probe **1** in the absence and presence of cyanide anions. Addition of one equivalent of cyanide ions to the fluorescent probe at room temperature causes significant upfield shifts of several different proton peaks, which include changes of doublet peaks corresponding to vinylic proton at the a-position from δ 8.10 ppm to δ 6.75 ppm, doublet peaks corresponding to vinylic proton at b-position from δ 6.96 ppm to δ 5.84 ppm, singlet peak corresponding to proton at g-position from δ 6.47 ppm to δ 6.22 ppm, doublet peaks corresponding to proton of indolium moiety at d-position from δ 7.84 ppm to δ 7.07 ppm, and doublet peaks related to proton of indolium moiety at c-position from δ 7.89 ppm to δ 6.67 ppm (Fig. 5), indicating the formation of the **1**-CN adduct. These upfield chemical shifts arise from the disappear-

ance of a positive charge in the fluorescent probe after the formation of the **1**-CN adduct, and are consistent with the formation of the cyanoindolium moiety by the nucleophilic attack of a cyanide anion to the iminium carbon. ^{1}H NMR analysis implied that the cyanide anion functions as a nucleophile in DMSO solution. Addition of more than one equivalent of cyanide does not cause any further chemical shift, implying that a 1 : 1 adduct between the probe **1** and CN$^-$ is formed. Job analysis for the addition reaction of the fluorescent probe with cyanide ions also corroborated the 1 : 1 binding stoichiometry (see Fig. S38 in the ESI†). The extinction coefficient of the fluorescent probe **1** is 6.8×10^4 M^{-1} cm^{-1} at 564 nm, and 5.7×10^4 M^{-1} cm^{-1} at 521 nm for the **1**-CN adduct.

We used different anionic species, such as F$^-$, Cl$^-$, Br$^-$, I$^-$, SCN$^-$, NO$_3^-$, CH$_3$COO$^-$, SO$_4^{2-}$, HSO$_4^-$, and H$_2$PO$_4^-$ to study the selectivity of probe **1** in the absence and presence of cyanide ions (Fig. 6, left). Among these various anion species tested, only cyanide ions respond to fluorescent probe **1** with large blue-shifts by 50 nm and 43 nm in the emission and absorption spectra, respectively (Fig. 6, left and Fig. S23–24 in the ESI†), and causes a remarkable visible color change from purple to pink (see Fig. S40 in the ESI†), and red to green in the absence and presence of a transilluminator, respectively. The presence of other anions, such as F$^-$, Cl$^-$, Br$^-$, I$^-$, SCN$^-$, NO$_3^-$, CH$_3$COO$^-$, SO$_4^{2-}$, HSO$_4^-$ or H$_2$PO$_4^-$, did not cause any significant change in the emission peak at 605 nm, but did result in a slight fluorescence enhancement at 515 nm, and a slight decrease in the absorption peak at 564 nm. The fluorescence ratio data (I_{555}/I_{605}) reveal that probe **1** is highly selective to cyanide anions over other common inorganic anions, which is due to the fact that cyanide is more nucleophilic than other anions in aqueous solution. These results indicate that fluorescent probe **1** may have a potential and promising application in the detection of cyanide ions in the presence of other different anions. Probes **2** and **3** also display a similar high selectivity towards cyanide ions over other anionic species (see Fig. 6, right and the ESI†).

In summary, we have successfully prepared selective and sensitive BODIPY-based probes for the ratiometric fluorescent
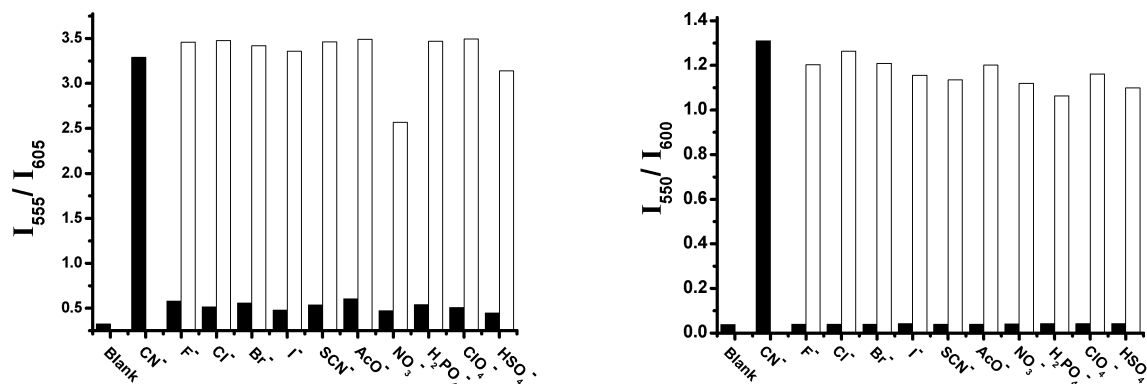

Fig. 6 The fluorescent ratiometric responses of probe **1** (left) (20 μM) and probe **3** (right) (20 μM) to different anions (100 μM) in the absence and presence of 60 μM and 90 μM cyanide ions in a mixed solution of CH$_3$CN and Tris buffer (10 mM, pH = 9.3) (9 : 1, v/v) and 100% Tris buffer (10 mM, pH = 9.3) respectively. Black bars show the fluorescent responses of the probes to different anions, while the white bars display the fluorescent responses of the probes to different anions in the presence of cyanide ion.

detection of cyanide ions. The highly water-soluble fluorescent probe **3** has a potential application in the detection of cyanide ions in aqueous solution.

Acknowledgements

References

1 S. I. Baskin and T. G. Brewer, in *Medical Aspects of Chemical and Biological Warfare*, TMM Publications, Washington, DC, 1997.

2 B. Vennesland, E. E. Comm, C. J. Knownles, J. Westly and F. Wissing, *Cyanide in Biology*, Academic Press, London, 1981.

3 P. K. Bhattacharya, *Metal Ions in Biochemistry*, Alpha Science International Ltd., Harrow, U.K., 2005.

4 C. Young, L. Tidwell and C. Anderson, *Cyanide: Social, Industrial, and Economic Aspects*, Minerals, Metals, and Materials Society, Warrendale, 2001.

5 J. L. Sessler and D.-G. Cho, *Org. Lett.*, 2008, **10**, 73–75.

6 X. Lv, J. Liu, Y. Liu, Y. Zhao, Y.-Q. Sun, P. Wang and W. Guo, *Chem. Commun.*, 2011, **47**, 12843–12845.

7 L. Yuan, W. Lin, Y. Yang, J. Song and J. Wang, *Org. Lett.*, 2011, **13**, 3730–3733.

8 K.-S. Lee, H. J. Kim, G.-H. Kim, I. Shin and J.-I. Hong, *Org. Lett.*, 2008, **10**, 49–51.

9 C.-L. Chen, T.-P. Lin, Y.-S. Chen and S.-S. Sun, *Eur. J. Org. Chem.*, 2007, 3999–4010.

10 Y. M. Chung, B. Raman, D. S. Kim and K. H. Ahn, *Chem. Commun.*, 2006, 186–188.

11 M. Jamkratoke, V. Ruangpornvisuti, G. Tumcharern, T. Tuntulani and B. Tomapatanaget, *J. Org. Chem.*, 2009, **74**, 3919–3922.

12 H. S. Jung, J. H. Han, Z. H. Kim, C. Kang and J. S. Kim, *Org. Lett.*, 2011, **13**, 5056–5059.

13 X. Lou, L. Qiang, J. Qin and Z. Li, *ACS Appl. Mater. Interfaces*, 2009, **1**, 2529–2535.

14 A. Loudet and K. Burgess, *Chem. Rev.*, 2007, **107**, 4891–4932.

15 Z. Ekmekci, M. D. Yilmaz and E. U. Akkaya, *Org. Lett.*, 2008, **10**, 461–464.

16 R. Ziessel, *C. R. Chim.*, 2007, **10**, 622–629.

17 R. Ziessel, G. Ulrich and A. Harriman, *New J. Chem.*, 2007, **31**, 496–501.

18 S. Zhu, J. Zhang, G. Vegesna, F.-T. Luo, S. A. Green and H. Liu, *Org. Lett.*, 2011, **13**, 438–441.

19 S. Zhu, J. Zhang, G. Vegesna, A. Tiwari, F.-T. Luo, M. Zeller, R. Luck, H. Li, S. Green and H. Liu, *RSC Adv.*, 2012, **2**, 404–407.

20 S. Zhu, J. Zhang, G. K. Vegesna, R. Pandey, F.-T. Luo, S. A. Green and H. Liu, *Chem. Commun.*, 2011, **47**, 3508–3510.

21 M. J. Frisch, G. W. Trucks, H. B. Schlegel, G. E. Scuseria, M. A. Robb, J. R. Cheeseman, G. Scalmani, V. Barone, B. Mennucci, G. A. Petersson, H. Nakatsuji, M. Caricato, X. Li, H. P. Hratchian, A. F. Izmaylov, J. Bloino, G. Zheng, J. L. Sonnenberg, M. Hada, M. Ehara, K. Toyota, R. Fukuda, J. Hasegawa, M. Ishida, T. Nakajima, Y. Honda, O. Kitao, H. Nakai, T. Vreven, J. A. Montgomery, J. E. Peralta, , F. Ogliaro, M. Bearpark, J. J. Heyd, E. Brothers, K. N. Kudin, V. N. Staroverov, R. Kobayashi, J. Normand, K. Raghavachari, A. Rendell, J. C. Burant, S. S. Iyengar, J. Tomasi, M. Cossi, N. Rega, J. M. Millam, M. Klene, J. E. Knox, J. B. Cross, V. Bakken, C. Adamo, J. Jaramillo, R. Gomperts, R. E. Stratmann, O. Yazyev, A. J. Austin, R. Cammi, C. Pomelli, J. W. Ochterski, R. L. Martin, K. Morokuma, V. G. Zakrzewski, G. A. Voth, P. Salvador, J. J. Dannenberg, S. Dapprich, A. D. Daniels, Ö. Farkas, J. B. Foresman, J. V. Ortiz, J. Cioslowski and D. J. Fox, *Gaussian 09*, Gaussian, Inc., Wallingford, CT, 2009.